Zero Voltage Switching over Entire Load Range and Wide Voltage Variation of Parallelly-Connected Dual-Active-Bridge Converter using Power-Circulating Operation

Hayato Higa and Jun-ichi Itoh
Department of Electrical Engineering
Nagaoka University of Technology
Niigata, Japan
hhiga@stn.nagaokaut.ac.jp, itoh@vos.nagaokaut.ac.jp

Abstract— **This paper proposes a power-circulating operation at light load operation for a parallelly-connected dual-active-bridge (DAB) converter in order to achieve zero voltage switching (ZVS) over entire load range and wide battery-voltage variation. At the light load, a power flow of each DAB converter is controlled in such a way that the transferred power of each DAB converter satisfies the condition for ZVS, i.e. the power-circulating operation. Consequently, MOSFET with low voltage rating can be used due to no surge voltage in ZVS. At the heavy load, the power-circulating operation is no longer required due to the high power flow of each DAB converter. The heavy load efficiency is not only improved but also the light load is operated without the recovery surge. From experimental results, at 75% of the nominal voltage, the ZVS range is extended by 380% compared to the ZVS range of only the same power flow operation. Moreover, the converter efficiency is over 95.6% from the rated power of 29% to the rated power at the nominal voltage.**

Keywords—Dual Active Bridge converter; Zero voltage switching; Parallel connection;

I. INTRODUCTION

Recently, energy storage systems have been actively installed to electric vehicles and DC micro-grid systems [1]. A bi-directional isolated DC-DC converter is used as the battery conversion systems. Due to its flexibility, a dual active bridge (DAB) converter is generally applied in such systems [2-3]. The DAB converter can obtain the high efficiency because zero voltage switching (ZVS) is achieved without additional components. ZVS not only reduces the turn-on loss but also reduces the surge voltage which occurs in the recovery mode of the body diode into MOSFET. As a result, the low voltage rating of MOSFET can be selected. However, the ZVS range is limited when the voltage fluctuates widely [3]. Due to the hard switching operation at the fluctuated voltage, the high voltage rating of MOSFET which has high on-state resistance has to be selected. Therefore, the converter efficiency at the heavy load region is decreased due to the worse performance of the high voltage rating of MOSFET. In addition, the error of the phase-shift angle occurs in the output voltage of the inverter which is the hard switching operation due to the dead-time error [4]. In the energy storage system, the DAB converter is operated in wide load range. Therefore, the extension of the ZVS range over entire load range is required with wide voltage range.

In order to extend ZVS range, the some modulation schemes have been presented [5-8]. Pulse width modulation is employed with the phase-shift control [5-6]. However, it is not always possible to achieve ZVS for all switches by the wide voltage range because the direction of the inductor current which discharges the junction capacitor cannot be controlled at the light load. On the other hand, pulse frequency modulation is applied depending on the voltage condition in order to keep the operation point at the ZVS condition [7-8]. However, the volume of the transformer becomes large because the volume of the transformer is decided by the minimum switching frequency. In a difference approach, the coupling coefficient of the transformer k_c is designed to be low [9]. However, due to large magnetizing current, the converter efficiency at the heavy load region decreases compared to that of the high coupling coefficient ($k_c \geq 0.99$).

In this paper, with the aiming for the extension of ZVS range over wide battery-voltage variation, the power-circulating operation of a parallelly-connected DAB converter is proposed. The original contribution in this paper is that the power-circulating operation of each DAB converter is used in order to achieve ZVS over entire load range and wide battery-voltage variation. In particular, when the power-circulating operation is active, the power flow of each DAB converter is changed in such a way that ZVS for all DAB converters is achieved. In addition, the low voltage rating of MOSFET can be selected because no surge voltage occurs in ZVS. This paper is organized as follows; firstly, the circuit configuration and the power-circulating operation are explained. Secondly, a flow chart to determine the power flow and the output power is introduced. Finally, the experiment is conducted in order to verify the ZVS operation at the light load with the variation of the battery voltage.

II. PROPOSED CIRCUIT

Fig. 1 shows the circuit configuration of the parallelly-connected DAB converter. By employing the parallel connection to the DAB converter, the conduction loss and the copper loss are reduced in compared to those when only one DAB converter is applied. However, the ZVS range is limited when the battery voltage fluctuates from the nominal voltage.

Fig. 2 shows the operation waveforms of each DAB converter. The transferred power is controlled in bidirectional direction by the phase angle between the high voltage (HV) side inverter and the low voltage (LV) side inverter.

Fig. 3 shows the power flow diagrams of the parallelly-connected DAB converter corresponding to the output power. Fig. 3(a) shows the parallel operation at heavy load where ZVS is simply achieved due to the high power flowing through each converter. Fig. 3(b) shows the single operation in which, only one DAB converter is operated under the ZVS condition of the each individual DAB converter with the parallel operation. Fig. 3(c) shows the power-circulating operation applied at light load. In the power-circulating operation, the power flow of each DAB converter is changed in order to achieve ZVS. The transferred power of each DAB converter P_1 and P_2 are designed to satisfy the condition for the ZVS achievement. It is noted that only two DAB converters are operated at light load because the transferred power P_1 will have to be increased if the number of the active converters increases. In other words, at light load, the No. 3~No. *m* DAB converter is inactive.

Fig. 4 shows the determination of the operation mode under condition that ZVS is achieved over entire load range. The operation mode is changed depending on the relationship between the reference transferred power P_{ref} and the lower limit of the transferred power for ZVS P_{ZVS}. The conditions based on P_{ref} and P_{ZVS} are explained as follows

- <u>Condition1: P_{ref}<P_{ZVS} Power-circulating operation</u>

When the condition 1 is met, ZVS is not achieved in each individual DAB converter if each DAB converter flows the same power in the same direction, i.e. the parallel operation or the single operation. Therefore, the power-circulating operation is used. In the power-circulating operation, the transferred power of each DAB converter P_1 and P_2 are adjusted to be larger than P_{ZVS}. As a result, the transferred power of each DAB converter P_1 and P_2 are calculated by (1).

$$\begin{aligned} P_1 &= P_{ref} + P_{ZVS} \\ P_2 &= -P_{ZVS} \end{aligned} \tag{1}$$

- <u>Condition 2: $P_{ZVS} \leq P_{ref} < 2P_{ZVS}$ Single operation</u>

In this condition, ZVS is achieved if only one DAB converter is active, i.e. the single operation. Therefore, only one DAB converter is operated. The other is operated that zero voltage is output in each inverter. In the single operation, the transferred power of each DAB converter P_1 and P_2 are calculated by (2).

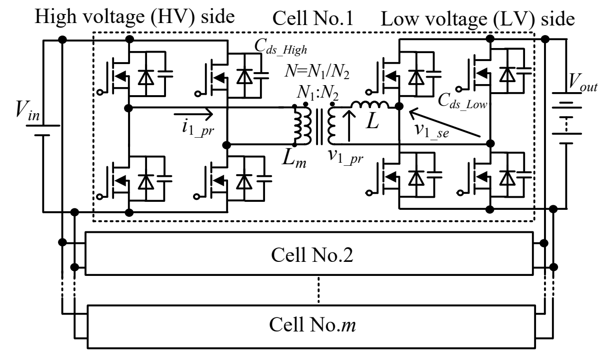

Fig. 1. Circuit configuration of parrallelly-connected DAB converter. The voltage of the HV side is 380V, whereas the voltage of the LV side varies from 36 V to 60 V.

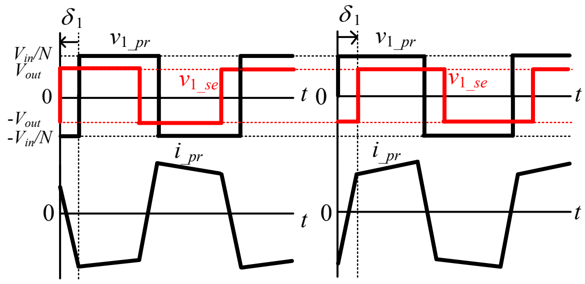

(a) Discharge operation (b) Charge operation

Fig. 2. Simplified waveforms of individually DAB converter The transferred power is controlled in bidirectional direction by the phase angle.

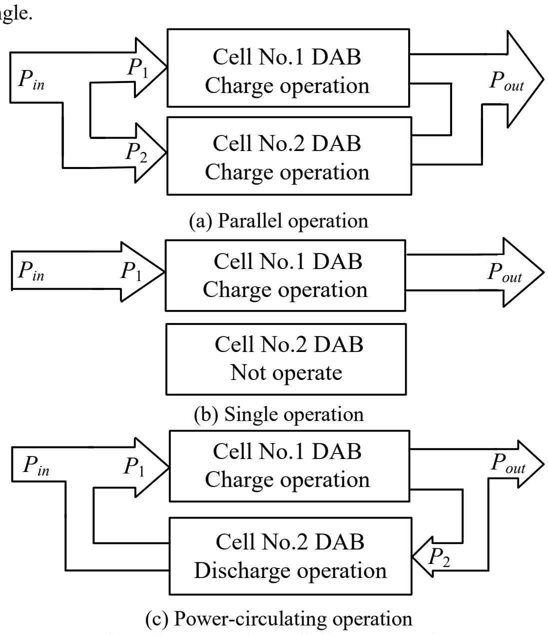

Fig. 3. Power flow diagrams of parrallelly-connected DAB converter. At heavy load where ZVS is simply achieved, the power flow of each DAB converter is the same. At light load, the power flow of each DAB converter is controlled in such a way that each DAB converter can still achieve ZVS.

$$\begin{aligned} P_1 &= P_{ref} \\ P_2 &= 0 \end{aligned} \tag{2}$$

- <u>Condition 3: $2P_{ZVS} \leq P_{ref} \leq P_{rated}$ Parallel operation</u>

In the condition 3, ZVS is achieved in each individual DAB converter. Therefore, the parallel operation is active. In the parallel operation, the transferred power of each DAB converter P_1 and P_2 are calculated by (3).

$$P_1 = P_{ref}/2 \\ P_2 = P_{ref}/2 \tag{3}$$

III. DERIVATION OPERATION MODE

This section introduces the flowchart, which derives the phase-shift angle of each DAB converter under the condition that ZVS is achieved over entire load range. Firstly, the dead time T_d is calculated by (4) in the wide ZVS range [10].

$$T_d = \frac{\pi}{2}\sqrt{LC_{ds}} \tag{4}$$

Fig. 5 shows the flowchart for deriving the transferred power of each DAB converter. If the parallel number is changed. The number of the operated DAB converters is changed depending on the reference of the transferred power. The ZVS condition is decided by the inductor current and the exciting current. In addition, the inductor current waveform is varied corresponding to the relationship among the input voltage, the output voltage and the power flow. At the condition of $NV_{out}>V_{in}$ the phase-shift angle of lower limit with ZVS condition δ_{ZVS} is calculated by (5) excluding the parasitic capacitance [3].

$$\delta_{ZVS} = \frac{\pi}{2}\left\{1 - \frac{2L_m}{2L_m + N^2 L}\frac{V_{in}}{NV_{out}} + 4\alpha f_{sw} T_d\right\} \tag{5}$$

At the condition of $NV_{out}<V_{in}$, the phase-shift angle of lower limit with ZVS condition δ_{ZVS} is calculated by (6) excluding the parasitic capacitance [3].

$$\delta_{ZVS} = \frac{\pi}{2}\left\{1 - \frac{2L_m + N^2 L}{2L_m}\frac{NV_{out}}{V_{in}} + 4\beta f_{sw} T_d\right\} \tag{6}$$

where α and β are coefficient which is decided by the power flow. The coefficient is decided to be α=1 β=-1 in the charge operation. On the other hand, the coefficient is decided to be α=-1 β=1 in the discharge operation. It should be noted that leakage inductance of the transformer is neglected when the phase-shift angle is calculated because the additional inductor L is much larger than the leakage inductance of the high frequency transformer. Then, the lower limit of the transferred power P_{ZVS} is calculated by (7) using δ_{ZVS}

$$P_{ZVS} = \frac{V_{in}V_{out}}{N\omega L}\delta_{ZVS}\left(1 - \frac{|\delta_{ZVS}|}{\pi}\right) \tag{7}$$

where ω is the switching angular frequency, N is transformer turn ratio. From (7), the references of the transferred power of each DAB converter P_{ref} are compared with P_{ZVS}. The parallel operation is active at the condition of P_{ref}>2P_{ZVS}. In contrast, the power-circulating operation is active at the condition of $P_{ref}<P_{ZVS}$. Next, the references transferred power of each DAB

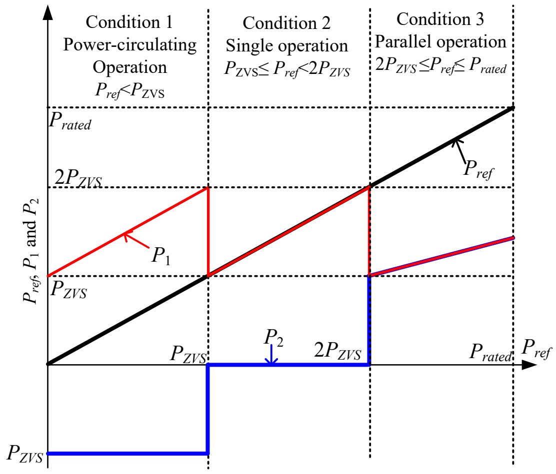

Fig. 4. Determination of operation mode depending on the reference transferred power P_{ref} in order to achieve ZVS over entire load range. In the light load condition of $P_{ref}<P_{ZVS}$, the power-circulating operation is active. The single operation is applied at the condition of $P_{ZVS} \leq P_{ref}<2P_{ZVS}$. In the heavy load of $2P_{ZVS} \leq P_{ref} \leq P_{rated}$, the parallel operation is employed. At the condition of $P_{ref}<0$, the power flows of P_1 and P_2 are switched.

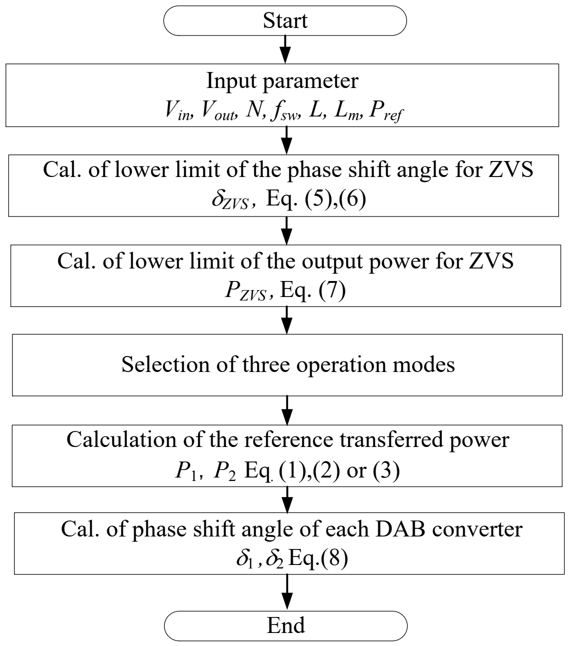

Fig. 5. Flowchart for deriving of transferred power under the condition that ZVS is achieved over entire load range

Table 1 Simlation condition

Input voltage V_{in}	380 V	Additional inductor L	2.19 µH
Output voltage V_{out}	36 V	Rated power	3 kW
Switching frequency f_{sw}	50 kHz	Magnetizing inductance L_m	3 mH
Dead-time T_d	100 ns	Turn ratio of transformer N	8
Parallelly connected number	2	Battery voltage range	36V to 60V
Parastic capacitance C_{ds_high}	200 pF	Parastic capacitance C_{ds_Low}	1200 pF

converter P_1, P_2 are calculated by (1), (2) or (3). Finally, the phase-shift angle δ_1, δ_2 are calculated by (8) [10].

$$\delta_1 = \frac{\pi}{2} - \sqrt{\frac{\pi^2}{4} - \frac{N\pi\omega L}{V_{in}V_{out}} P_1} \tag{8}$$

IV. SIMULATION RESULTS

In this section, the simulation results are demonstrated in order to evaluate the power-circulating operation. Table 1 shows the simulation conditions. The parallel number of DAB converter is two. It is noted that the output power which ZVS is achieved is 875 W from Eq. (5) and (6).

Fig. 6 shows the output voltage of each inverter v_{1_pr}, v_{1_se}, v_{2_pr}, v_{2_se} and the inductor current at the HV side i_{1_pr}, i_{2_pr} when the power-circulating operation is active at the output power of about 205 W, i.e. the power which cannot achieve ZVS for each individual DAB converter. It is confirmed that the output power of 205 W at light load can be generated by changing the transferred power and the power flow of each DAB converter.

Fig. 7 shows waveforms of the gate signal and drain-source voltage with the power-circulating operation and the parallel operation. In Fig. 7(a), hard switching is confirmed because MOSFET is turned on at the output voltage V_{out}. In Fig. 7(b), The ZVS operation is confirmed by the power-circulating operation because MOSFET of each inverter are turned on at the zero voltage. Therefore, ZVS at light load is achieved by power-circulating operation.

Fig. 8 shows characteristics of the input power P_{in} and the reference transferred power P_{ref}. The ZVS range is extended by 110% compared to the parallel operation. The ZVS achievement not only reduces the switching loss but also eliminates the dead-time error of the phase-shift angle. Therefore, compared to when using only the parallel operation, the error between the input power and the reference transferred power is reduced to 12 % by using the power-circulating operation.

V. EXPERIMENTAL RESULTS

Table 2 shows the experimental parameters. A 1.5 kW prototype of two parallelly-connected DAB converter is tested in order to confirm the validity of the power-circulating operation. When the output voltage is 36 V, the lower limit of transferred power for ZVS P_{ZVS} is 411 W with the single operation. When the output voltage is 48 V, ZVS is achieved over entire load range at the charge operation. Therefore, the power-circulating operation is inactive at the nominal voltage. It is noted that the additional inductor is connected in series to LV side of the high frequency transformer. In the LV-side inverter of MOSFET, IRFP4110PbF (Infenion) is selected. IRFP4110PbF has the on-state resistance R_{on} =3.7 mΩ, the voltage rating V_{rate}=100 V and the current rating I_{rate}=120A. On the other hand, SCT3030AL-E (Rohm) is selected at the HV-side inverter. SCT3030AL-E has the on-state resistance R_{on} =30 mΩ, the voltage rating V_{rate}=650 V and the current rating I_{rate}=70A.

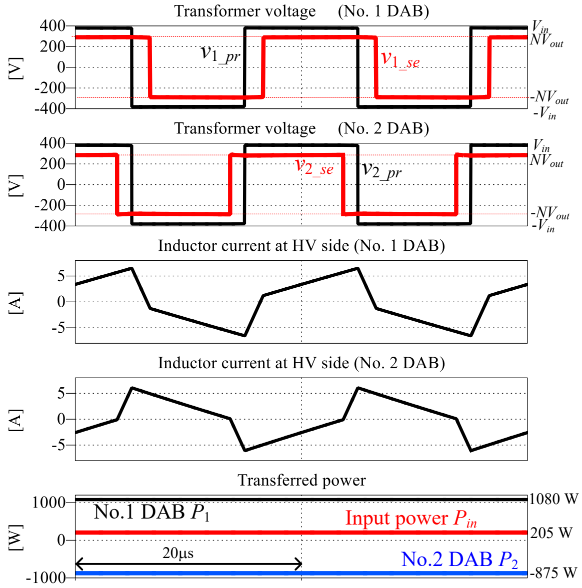

Fig. 6. Operation waveforms with power-circulating operation. The lower limit of the output power for ZVS condition is 875 W. The light load operation is confirmed even with the power-circulating operation.

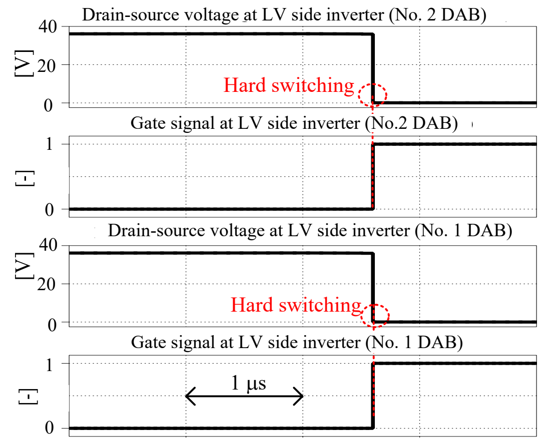

(a)Parallel operation(P_{out}=380 W)

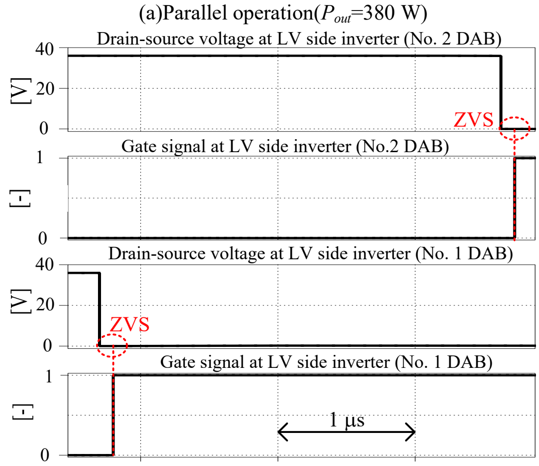

(b) Power-circulating operation (P_{out}=205 W)

Fig. 7. Waveforms of gate signal and drain-source voltage. With applying the only parallel operation, ZVS is not achieved. Furthermore, the recovery surge in MOSFET occurs. On the other hand, ZVS is achieved by using the power-circulating operation, which results in no turn-on loss.

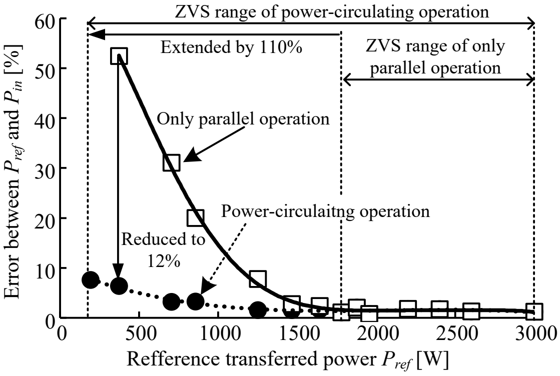

Fig. 8. Characteristics of reference transferred power and error between input power P_{in} and reference transferred power P_{ref}. The ZVS range is exrtended by 110%. In addition, the error between P_{in} and P_{ref} is reduced to 12%.

Fig. 9 shows the operation waveforms with three operations at 380 V of the input voltage and 36 V of the output voltage. Fig. 9 (a) shows that of the parallel operation at the output power of 1048 W. Fig. 9 (b) shows that of the single operation at the output power of 542 W. Fig. 9 (c) shows that of the power-circulating operation at 235 W, i.e. the achievement of ZVS in each individual DAB converter. In Fig. 9 (a), the parallel operation is confirmed at the same power flow. As a result, the conduction loss and copper loss can be reduced in compared to only single operation. In Fig. 9(b), the single operation is confirmed because only one DAB converter is operated. On the other hand, the power-circulating operation is obtained because the each individual DAB converter is difference power flow. In three operations, the transferred power of the each individual DAB converter P_1 and P_2 are over the lower limit of the transferred power P_{ZVS}. By using the power-circulating operation, the light load operation is not used in the each individual DAB converter. As a result, the ZVS is achieved over entire load range.

Fig. 10 shows operation waveforms of the gate signal and the drain-source voltage with/without the power-circulating operation. Fig. 10(a) shows that with parallel operation. Fig. 10(b) shows that with the power-circulating operation. In Fig. 10(a), the hard switching is confirmed that MOSFET is turned on at the output voltage. Furthermore, the high voltage surge occurs in MOSFET due to the recovery mode. In Fig. 10(b), ZVS is confirmed because MOSFET is turned on at the zero voltage. Therefore, the high voltage rating of MOSFET is not required because the recovery surge is avoided by the power-circulating operation. It is noted that the turn-off loss can be reduced by connecting snubber capacitors in parallel to MOSFET in order to delay the rise of the drain-source voltage

Fig.11 shows efficiency characteristics of two parallelly-connected DAB converter. Fig. 11(a) shows that when the output voltage is 48 V and the input voltage is 380 V, i.e. the nominal voltage. Fig. 11(b) shows that when the output voltage is 36 V and the input voltage is 380 V. In Fig. 11(a), the light load efficiency is improved by using the single operation because the iron loss is reduced by no operation of one DAB converter. Therefore, the converter efficiency is over 95.6% from the rated power of 29% to the rated power by changing the

Table 2 Experiment condition

Input voltage V_{in}	380 V	Additional inductor L	2.03 µH
Output voltage V_{out}	36, 48 V	Rated power	1.5 kW
Switching frequency f_{sw}	100 kHz	Magnetizing inductance L_m	1.6 mH
Dead-time at HV side	100 ns	Turn ratio of transformer N	N_1/N_2=15/2
Dead-time at LV side	150 ns	Parallely connected number	2
Parastic capacitance C_{ds_Low}	100 pF	Parastic capacitance C_{ds_Low}	400 pF

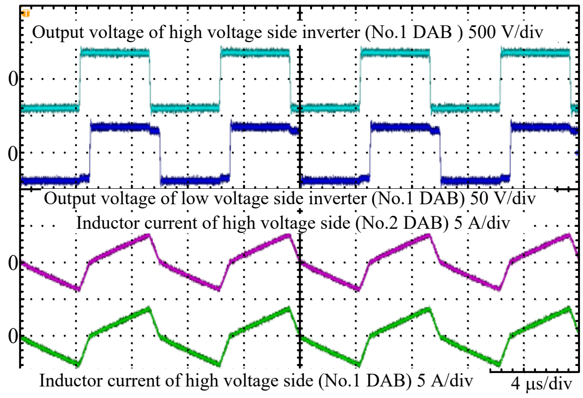

(a) Parallel operation at 1048 W

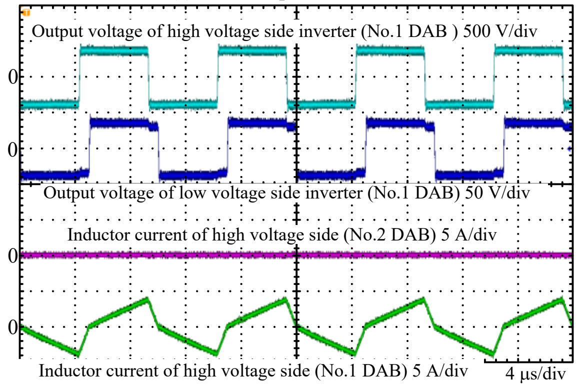

(b) Single operation at 542 W

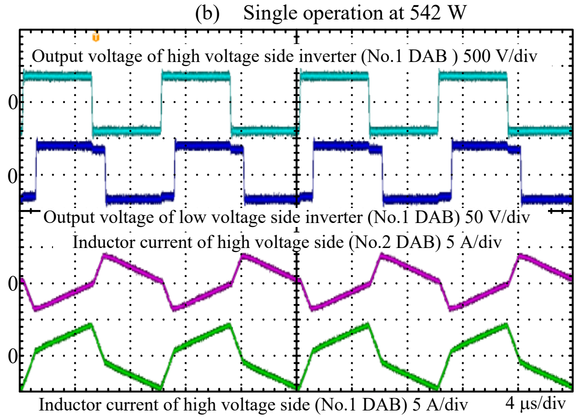

(c) Power-circulating operation at 235 W

Fig. 9. Operation waveforms for two parallelly-connected DAB converter. Three operations are confirmed by changing the power flow of the each individual DAB converter. In the power-circulating operation, the transferred power of the each individual DAB converter P_1 and P_2 are 805 W, 537 W, i.e. the ZVS achievement in the each individual DAB converter.

power flow of the each DAB converter depending on the output power. In addition, the ZVS is achieved over entire load range. In Fig. 11(b), the ZVS range is extended by 380% compared with only the parallel operation. In addition, the maximum efficiency 96.2% is achieved. However, the light load efficiency is low by the power-circulating operation because the conduction loss and copper loss is increased due to large the lower limit of the transferred power. In order to improve the converter efficiency with the power-circulating operation, the design of the magnetizing inductance L_m and the additional inductance L are important from (5), (6).

VI. Conclustion

This paper proposed the power-circulating operation for the parallelly-connected DAB converter with the aiming of achieving ZVS over entire load range and wide battery-voltage variation. In the proposed method, the power flow and the transferred power were changed depending on the output power in order to operate all DAB converters at the ZVS condition. In the experimental results, the ZVS range was extended by 380% compared to that when using only parallel operation. At the nominal voltage, the converter efficiency is over 95.6% from 29% the rated power to the rated power by changing the power flow of the each individual DAB converter. In the future work, the design of the magnetic components will be consider in order to achieve the high efficiency in wide load.

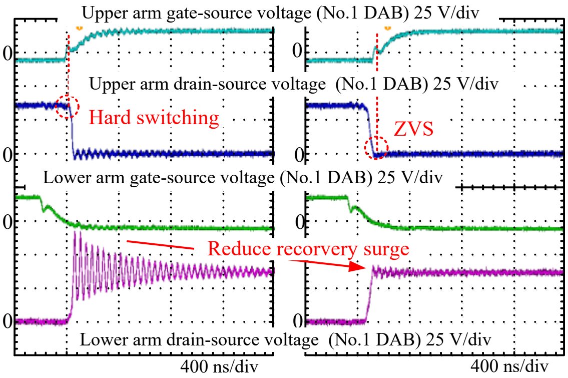

(a) Without circulating operation (b) With circulating operation

Fig. 10. Waveforms of gate signal and drain-source voltage at light load. In Fig. (a), ZVS is not achieved when the power-circulating operation is not applied, whereas ZVS is achieved if the power-circulating operation is applied, which results in no turn-on loss. In addition, the turn-off loss can be reduced by connecting a snubber capacitor parallel to MOSFET.

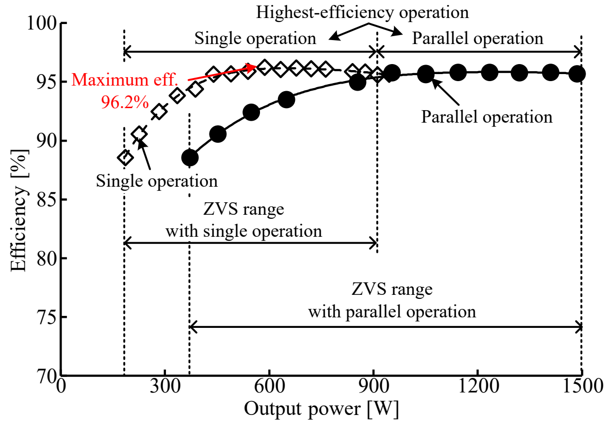

(a) V_{in}=380 V, V_{out}=48 V (Nominal voltage)

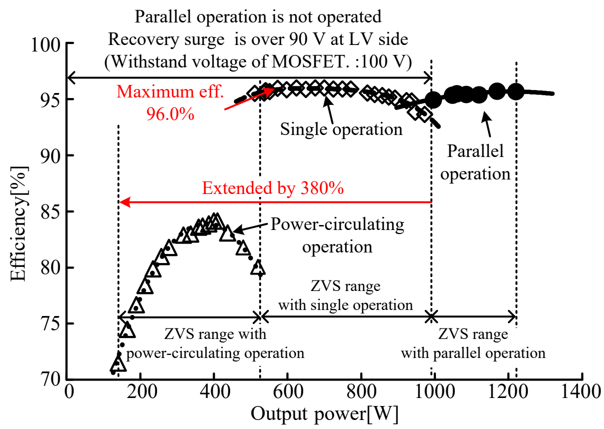

(b) V_{in}=380 V, V_{out}=36 V (75% nominal voltage)

Fig. 11. Efficiency characteristics of two parallelly-connected DAB converter with fluctuation of output voltage. At the nominal voltage, the light load efficiency is improved by the single operation compared with only parallel operation. The maximum efficiency is 96.2% at 678 W. At 75% of the nominal voltage, ZVS range is extended by 380% compared with only parallel operation. In addition, the parallel operation at the light load is not operated because the surge voltage in MOSFET is 90 V due to the recovery mode.

References

[1] Meiqin Mao, etc. "Accurate Output Power Control of Converters for Microgrids Based on Local Measurement and Unified Control", IEEJ Journal of Industry Applications, Vol. 4, No. 4, pp.331-338, 2015.

[2] R. W. D. Doncker, etc. "A three-phase soft-switched high-power-density dc/dc converter for high-power applications", IEEE Trans on Industry Applications, Vol, 27, No. 1, pp. 63-73, 1991.

[3] Kheraluwala M.N, etc :"Preformance Characterization of a High Power Dual Active Bridge dc-to-dc Converter", IEEE Trans. I.P., Vol. 28, No. 6, pp. 1294-1301, 1992.

[4] Biao Zhao, etc.: "Dead-Time Effect of the High-Frequency Isolated Bidirectional Full-Bridge DC–DC Converter: Comprehensive Theoretical Analysis and Experimental Verification", IEEE Trans. PELS., Vol. 29, No. 4, pp. 1667-1680, 2014.

[5] Yoichi Ishizuka, etc, "Static Characteristic Analysis of Proposed Bi-Directional Dual Active Bridge DC-DC Converter", IEEJ Journal of Industry Applications, Vol.4,No. 5, pp.602-610, 2015.

[6] Florian Krismer, Johann W. Kolar: "Closed Form Solution for Minimum Conduction Loss Modulation of DAB Converters", IEEE Trans. PELS., Vol. 27, No. 1, pp. 174-188, 2012

[7] Xiao-Fei He, etc., "A Variable Switching Frequency Hybrid Control for ZVS Dual Active Bridge Converters to Achieve High Efficiency in Wide Load Range", APEC2014 , Vol. , No. , pp. 1095-1099, 2014

[8] Felix J and Jurgen B, "Generalized Modeling and Optimization of a Bidirectional Dual Active Bridge DC-DC Converter Including Frequency Variation", IEEJ Journal of IndustryApplications, Vol.4, No.5, pp.593-601, 2015.

[9] J. Riedel, etc: "Wide Range ZVS Operation of Dual Active Bridge DC-DC Converter using Adaptive Modulation and Low Coupling Factor Transformers", EPE2016, 2016.

[10] Hirofumi Akagi, etc.:"Power-Loss Breakdown of a 750-V 100-kW 20-kHz Bidirectional Isolated DC–DC Converter Using SiC-MOSFET/SBD Dual Modules", IEEE Trans.IAS., Vol. 51, No. 1, pp. 420-428, 2015